Disrupted dynamic functional connectivity in distinguishing subjective cognitive decline and amnestic mild cognitive impairment based on the triple-network model

Chen Xue
Nanjing Brain Hospital
Wenzhang Qi
Nanjing Brain Hospital
Qianqian Yuan
Nanjing Brain Hospital
Guanjie Hu
Nanjing Brain Hospital
Honglin Ge
Nanjing Brain Hospital
Jiang Rao
Nanjing Brain Hospital
Chaoyong Xiao
Nanjing Brain Hospital
Jiu Chen (ericcst@aliyun.com)
Nanjing Medical University https://orcid.org/0000-0001-8185-8575

Research

Keywords: subjective cognitive decline, amnestic mild cognitive impairment, dynamic functional connectivity, resting state functional magnetic resonance imaging

Posted Date: April 9th, 2021

DOI: https://doi.org/10.21203/rs.3.rs-394271/v1

Abstract

Background

Subjective cognitive decline (SCD) and amnestic mild cognitive impairment (aMCI) were wildly thought to be preclinical AD spectrum, who characterized by aberrant functional connectivity (FC) within the triple networks involving the default mode network (DMN), the salience network (SN), and the executive control network (ECN). Dynamic FC (DFC) analysis can capture the temporal fluctuation of brain FC during the scan that static FC analysis cannot provide. The purpose of the current study was to explore the changes of dynamic FC within the triple networks of preclinical AD spectrum, and further reveal its potential diagnostic value in the preclinical AD spectrum.

Methods

We collected resting-state functional magnetic resonance imaging data from 44 SCD, 49 aMCI, and 58 controls (HC). DFC analysis based on the sliding time-window correlation method were used to analyze the DFC variability within the triple networks among three groups. Then the correlation analysis was conducted to reveal the relationship between the altered DFC variability within the triple networks and the declined cognitive function. Furthermore, the logistic regression analysis was used to assess the diagnostic accuracy of altered DFC variability within the triple networks in SCD and aMCI.

Results

Compared to HC, SCD and aMCI both showed altered DFC variability within the triple networks. The DFC variability in the right middle temporal gyrus and left inferior frontal gyrus (IFG) within ECN were significantly different between SCD and aMCI. Moreover, the altered DFC variability in the left IFG within ECN was obviously associated with the decline in episodic memory and executive function. Last but not least, the logistic regression analysis showed multivariable analysis had high sensitivity and specificity in the diagnosis of SCD and aMCI.

Conclusions

SCD and aMCI showed similar and distinct trends in the DFC variability within the triple networks and the altered DFC variability within ECN involved episodic memory and executive function. More importantly, the altered DFC variability and triple-network model proved to be an important biomarker to diagnosis and identification of preclinical AD spectrum.

Introduction

Alzheimer's disease (AD) is a great medical challenge that haunts the world because of its progressive, irreversible and incurable nature, so subjective cognitive decline (SCD), as its preclinical stage, and amnestic mild cognitive impairment (aMCI), as its prodromal stage, have received more attention [1–4]. SCD, which refers self-report memory decline in the elderly with normal objective cognitive performance, is widely believed to have twice times to give rise to aMCI/AD than elderly without SCD [2, 5]. aMCI, which is characterized by subjective memory decline, is thought to be nearly 10 times to progress to AD than healthy elderly [2, 6–8]. However, the disease mechanism of AD spectrum still remains unknown. Therefore, it is crucial to investigate the shared and specific brain function network alternation of SCD and aMCI to promote the understanding the pathophysiology of preclinical AD spectrum.

Resting-state functional magnetic resonance imaging (rsfMRI), which is a task-independent and powerful imaging modality, has been widely used in the intrinsic functional connectivity networks of neuropsychiatric diseases [9, 10]. Of many intrinsic brain networks, the triple-network model, composed of the default-mode network (DMN), salience network (SN), and executive control network (ECN), aroused great concern in recent researches [11–13]. The DMN, mainly located in the ventromedial prefrontal cortex (vmPFC) and posterior cingulate cortex (PCC), is activated for internally directed cognitive activities, such as self-referential mental processes and social functions [14, 15]. The ECN, primarily involved in the lateral posterior parietal cortex (PPC) and dorsolateral prefrontal cortex (dlPFC), is activated during externally directed higher-order cognitive function, including working memory, decision-making, and attention [16]. The SN, which primarily include the anterior cingulate cortex (ACC) and anterior insula, is associated with affective processes, attention, and interoceptive [17, 18]. Specifically, when salient events are detected, the SN can activate brain networks, direct DMN and ECN to perform cognitive tasks, and help corresponding brain regions to respond to stimuli appropriately [11, 19]. Numerous researches have suggested that the triple networks can be used to detect the reliability and stability of large-scale connections mode and have damage in neuropsychiatric diseases [13, 20–22]. Further study of the triple-network model alternation in SCD and aMCI could help us better understand their pathological mechanisms.

Many neuroimaging studies have demonstrated that SCD and aMCI showed altered functional connectivity (FC) in the triple networks [21, 23, 24]. However, all the aforementioned researches were based on the assumption that the functional networks are spatiotemporally static during the MRI scan [25]. Due to the complexity and the changing environment of the human brain, the assumption that brain activity remains static is too simplistic and may lose the dynamic characteristics of brain activation and connectivity [26]. The dynamic FC (DFC) analysis has become a hotspot in rsfMRI researches to capture the temporal fluctuation of brain FC during the scan [27]. Previous researches have demonstrated that quantification of dynamic FC disruption might be a sensitive biomarker and/or prognostic indicator of disease progression and cognitive function [28, 29]. Moreover, some studies have highlighted the potential role of DFC analysis in improving the accuracy of disease diagnosis, which made it necessary to apply DFC analysis to AD spectrum diagnosis [30].

A number of researches has found that AD showed altered DFC. Gu.et.al., suggested that AD showed decreased regional temporal variability primarily in the temporal, parietal, and somatomotor regions [31]. The authors also found that disrupted DFC was associated with cognitive function in AD patients. They claimed that the DFC analysis provided novel into the pathophysiological mechanisms of AD. In recent years, the research focus has been shifted to preclinical AD spectrum, including SCD and MCI. Córdova-Palomera et.al. suggested that AD patients showed altered DFC mainly in frontal-superior, temporal, and default-mode compared to MCI [32]. Niu et.al. found that aMCI patients showed altered DFC in the prefrontal and parietal cortexes compared to HC and the regions were majorly in the DMN [33]. Dong et.al. found that SCD showed both increased and decreased temporal variability compared to HC [34]. However, previous studies had not revealed the changes of DFC with the progression of preclinical AD spectrum. It is unclear whether there are common and/or specific changes in DFC features in SCD and aMCI. Especially there are few researches on the alternation of DFC variability within the triple networks in SCD and aMCI and its diagnosis value in SCD and aMCI.

Therefore, in the current study, combined rsfMRI and classic sliding time-window correlation (SWC) approach, we aimed to reveal the DFC variability changes within the triple networks in SCD and aMCI, as well as the relationship with cognitive function. In addition, we further explored diagnostic efficiency of DFC variability in SCD and aMCI. We hypothesized that there were similar and distinct disruptions of the DFC variability within the triple networks in SCD and aMCI and altered DFC variability of triple networks may contribute to cognitive decline. Additionally, the comprehensive analysis of DFC temporal variability within triple networks can be served as a terrific indicator to diagnose and identify SCD and aMCI.

Materials And Methods

Subjects

The applied research data were obtained from our in-home database: Nanjing Brain Hospital-Alzheimer's Disease Spectrum Neuroimaging Project (NBH-ADsnp) (Nanjing, China), which is continuously being updated. Related information of the NBH-ADsnp was summarized in *SI Methods*. The research gained approval by the responsible Human Participants Ethics Committee of the Affiliated Brain Hospital of Nanjing Medical University (No. 2018-KY010-01 and No. 2020-KY010-42). All volunteers participate voluntarily and with written informed consent. The current study used 151 data (until January 21, 2020) including 58 healthy control (HC), 44 SCD, and 49 aMCI from the NBH-ADnsp database. The inclusion and exclusion criteria of participants were provided in *SI Method*. All subjects underwent a comprehensive and standardized clinical evaluation interview including demographic inventory, medical history, neurological and mental status examination, and MRI scan.

Neurocognitive assessments

Classical and comprehensive neurocognitive assessments were performed for all participants, including general cognitive functions, episodic memory, executive function, information processing speed, and visuospatial function. Details regarding the neurocognitive assessments were summarized in *SI Method.*

MRI data acquisition

The details regarding image acquisition parameters (structure MRI images and rsfMRI images) are provided in *SI Methods.*

Preprocessing of rsfMRI data

The functional MRI images were analyzed as described in precious study using the DPABI based on SPM program, implemented in MATLAB2013b with the following steps [35, 36]: We discarded the first 10 volumes and performed the slice timing correction and head motion correction. Participants with excessive head motion (cumulative translation or rotation > 3.0 mm or 3.0^0) were excluded. Subsequently, segmentation and nuisance covariate regression with 24 motion parameters, global signal, white matter signal, and cerebrospinal fluid signal were performed. Then, we selected the filtering frequency at 0.01–0.08 Hz, used T1 image unified segmentation for normalization, and resampled to an isotropic voxel size of 3 mm. Finally, we applied spatial smoothing with a 6-mm FWHM Gaussian kernel and detrending.

After preprocessing, we further processed the preprocessed data according to the following steps illustrated in Fig. 1.

Definition of Functional Brain Networks

Seed-based static FC analysis was carried out to extract the triple networks. In the current study, four 10-mm spherical regions of interest (ROIs) centered in the ventromedial prefrontal cortex (vmPFC; MNI space: 0, 52, -6) for the anterior DMN (aDMN), posterior cingulated cortex (PCC; MNI space: 0, -53, 26) for posterior DMN (pDMN), right anterior insula (rAI; MNI space: 38, 22, -10) for the SN, and right dorsolateral prefrontal cortex (DLPFC; MNI space: 48, 12, 34) for the ECN were created according to previous studies [3, 37, 38]. The averaged time series of ROIs of each participates were extracted, and a voxel-wise cross-correlation analysis was conducted between the averaged time series within the ROIs and the whole brain within the GM mask. A Fisher's *z*-transformation was applied to enhance the normality of the correlation coefficients.

Following this, the individual correlation maps from the HC group were subjected to a random-effect analysis by using one-sample t-test. The threshold was set at $p < 0.05$ with threshold-free cluster enhancement (TFCE) approach (1,000 random permutations) family-wise error (FWE) corrected. The regions which positively functional connections to the four ROIs were defined as templates for aDMN, pDMN, SN, and ECN.

.

Seed-based DFC Variability within the Triple Networks

The dynamic brain connectome analysis toolbox (http:// restfmri.net/forum/DynamicBC) was performed to compute DFC variability within the aDMN, pDMN, SN, and ECN. Firstly, similar to above static FC

analysis, seed-based (vmPFC, PCC, rAI, and DLPFC) voxel-wise dynamic FC was applied to calculate DFC changes of the triple networks. The most classic sliding time-window correlation (SWC) method was used to compute the correlation between each ROI with a width of 40 TRs slid in steps of 2 TR according to previous studies, resulting in the analysis of 96 windows [39, 40]. For each obtained a correlation coefficient, which was converted to z scores by the Fisher r-to-z transformation to improve normality. These Fisher's z-transformed correlation results were used to further calculate the temporal variation of DFC.

Statistical analysis

The Statistical Package for the Social Sciences (SPSS) software version 22.0 (IBM, Armonk, New York, NY, USA) was performed to analyze demographic and clinical information. Analysis of variance (ANOVA) and the chi-square test were conducted to compare the demographic and neurocognitive data across three groups, including SCD, aMCI, and HC. Bonferroni correction with p value < 0.05 were used for post-hoc analysis.

One-way ANOVA was used to compare the differences in DFC variability in the aDMN, pDMN, SN, and ECN within corresponding network mask among three groups, including SCD, aMCI, and HC, after controlling the effects of age, gender, and years of education. The non-parametric permutation test with the permutation times at 1,000 was performed in the present study to precisely control the false positive rate. The corrected $p < 0.05$ and the cluster number ≥ 20 voxels (cluster size ≥ 540 mm^3) were applied to multiple comparisons. The two-sample t-test was used for post-hoc comparisons with the mask resulted from the ANOVA analysis with age, gender, and years of education as covariates. The significance level was set with a TFCE-FWE corrected $p < 0.05$ and the cluster number > 9 voxels (cluster size > 243 mm^3).

The significantly altered DFC variability was extracted with the DPABI and used for the next correlation analysis. The correlation analysis was conducted by SPSS software to explore the relationship between altered DFC variability and cognitive domains with age, gender, and years of education as covariates (Bonferroni corrected, $p < 0.05$).

Binary Logistic Regression Analysis

Univariate and multivariable analysis of binary logistic regression were conducted in SPSS software to test the diagnosis value of DFC variability in SCD and aMCI. Altered DFC variability and cognitive function in the univariate analysis were included in the multivariable models by using backward elimination according to the likelihood ratio with a variable selection criterion of $p < 0.05$. We estimated the receiver operating characteristic (ROC) curve and the area under the receiver operating characteristic curve (AUC) to assess the predictive ability of the univariate and multivariable models, manifested in the accuracy, sensitivity, and specificity. A p value < 0.05 was considered statistically significant.

Results

Demographic and neurocognitive characteristics

The demographic and neurocognitive characteristics of all subjects, including 49 aMCI, 44 SCD, and 58 HC, were exhibited in Table 1. As is expected, the results showed significant differences in cognitive performance. The aMCI group showed significant lower episodic memory, and executive function scores compared to both SCD and HC groups. aMCI group showed significantly lower information processing speed and visuospatial function compared to HC (Bonferroni corrected for post-hoc, $p < 0.05$).

Altered DFC variability of triple networks in SCD and aMCI

In the aDMN subnetwork, the ANOVA analysis showed significantly altered DFC variability among three groups, including right parahippocampal gyrus, right inferior frontal gyrus (IFG), left anterior cingulum gyrus, left caudate, right angular gyrus, right superior temporal gyrus (STG), and bilateral superior frontal gyrus (SFG). Compared to HC, aMCI showed decreased DFC variability in right angular and right SFG (TFCE-FWE corrected, $p < 0.05$, cluster number > 9 voxels). All results were obtained with age, gender, and years of education as covariates (see Table 2 and Fig. 2).

In the pDMN subnetwork, the ANOVA analysis showed significantly altered DFC variability in right middle temporal gyrus (MTG) among three groups. Compared to HC, SCD showed significant decreased DFC variability in right MTG (TFCE-FWE corrected, $p < 0.05$, cluster number > 9 voxels). All results were obtained with age, gender, and years of education as covariates (see Table 2 and Fig. 2).

In the SN, the ANOVA analysis showed significantly altered DFC variabilityin left hippocampus, right IFG, left insula, left putamen, left STG, and right IFG. Compared to HC, aMCI showed increased DFC variability in left putamen while SCD showed increased DFC variability in left putamen and left insula (TFCE-FWE corrected, $p < 0.05$, cluster number > 9 voxels). All results were obtained with age, gender, and years of education as covariates (see Table 2 and Fig. 3).

In the ECN, the ANOVA analysis showed significantly altered DFC variability in bilateral MFG, left IFG, and right inferior parietal lobule. Compared to HC, SCD showed increased DFC variability in MFG. Compared to SCD, aMCI showed decreased DFC variability in right MFG while increased DFC variability in left IFG (TFCE-FWE corrected, $p < 0.05$, cluster number > 9 voxels). All results were obtained with age, gender, and years of education as covariates (see Table 2 and Fig. 4).

Behavioral significance of altered DFC variability within triple networks in SCD and aMCI

The correlation analysis showed that in the groups consisting of SCD and aMCI, the altered DFC variability in the left IFG of ECN was significantly negative correlated to EM ($r = -0.421$, $p < 0.001$) and EF ($r = -0.382$, $p < 0.001$) (Bonferroni corrected, $p < 0.05$). Age, gender, and years of education were used as covariates for all these results (see Fig. 4).

Diagnosis and classification of SCD and aMCI using the logistic regression analysis

The ROC curve of each altered indexes was shown in Fig. 5. Obviously, the best-fitting model was based on the multivariable models combining altered DFC variability and declined cognitive function. The AUC of SCD and HC based on the multivariable model was 0.877, with 88.6% sensitivity, and 75.9% specificity ($p < 0.001$). In the group of aMCI and HC, the AUC based on the multivariable model was 0.927, with 75.0% sensitivity, and 98.2% specificity ($p < 0.001$). Last but not least, the AUC of SCD and aMCI based on the multivariable model was 0.907, with 86.4% sensitivity, and 81.8% specificity ($p < 0.001$).

Discussion

To our best, the present study was the first study analyzing the DFC variability of SCD and aMCI patients based on the triple-network model and the association with cognitive decline. The primary findings of the study were that SCD and aMCI had similar and distinct change pattern of DFC variability within the triple networks. Moreover, altered DFC variability within ECN has been found to be significantly correlated to cognitive performances in SCD and aMCI. Most important of all, altered DFC variability combined with the triple-network model can serve as an important biomarker for their higher diagnostic efficiency of SCD and aMCI.

The present study showed that the DFC variability within the triple networks, including DMN, SN, and ECN, has changed to different degrees in the SCD and aMCI. Actually, the DMN can be divided into aDMN and pDMN, and has been considered to be independent in a wide range of cognitive tasks. To be specific, the aDMN is involved in self-referential mental idealization while the pDMN in episodic memory retrieval [41]. In the present study, SCD showed decreased DFC variability in the right MTG within pDMN compared to HC while aMCI showed decreased DFC variability in the right angular gyrus and right SFG within the aDMN. The impaired brain regions are involved in functions of language processing (angular gyrus), spatial orientation (angular gyrus), motor planning and executive (SFG), and visual information (MTG). This might mean that impairment in DMN may lead to extensive cognitive decline. Moreover, a prior static FC study indicated that the FC of aDMN first increased and then decreased with progression of AD spectrum disease, which was consistent with our results that DFC variability of aDMN was decreased in aMCI compared to HC while SCD remained stable [41]. Notably, the previous DFC studies demonstrated that higher DFC variability of brain regions may reflect greater complexity and greater ability in information processing [42]. Decreased DFC variability may indicate decreased information processing ability of SCD and aMCI [42]. The decreased DFC variability within DMN subnetworks of SCD in the present study means that SCD already had the potential tendency of impaired information processing ability. In addition, SCD showed altered DFC variability majorly in pDMN while aMCI showed altered DFC variability mainly in aDMN, which seemed to confirmed the specificity of AD spectrum in DFC variability within DMN.

In our study, the SCD and aMCI groups both showed increased DFC variability in the left putamen within SN, while aMCI additionally showed increased DFC variability in the left insula within SN. The putamen is part of neostriatum, which was identified as one of the first brain areas affected by amyloid deposition in healthy elderly [43]. Previous studies regarded that the putamen involves in the working memory and probabilistic learning and might be an appropriate clinical biomarker for neurodegenerative disease [44, 45]. Research reported that the decline of ALFF and volume in putamen was significantly related to cognitive decline in AD spectrum [46, 47]. The insula, a major region of SN, is believed to play an important role in the maintenance of memory performance in the early stage of the AD spectrum [48]. One study suggested that the left insula has the higher node degree and participation coefficient in the brain network and associated to episodic memory [41]. Increased DFC variability of SN in patients verified the “brain reserve” hypothesis that enhanced FC of SN in SCD and aMCI might be a compensatory mechanism for the decreased DMN function so that it can resist amyloid protein deposition and maintain relatively normal cognitive function [22, 49].

Our results showed that the altered DFC variability within ECN in SCD and aMCI. ECN, with the prefrontal lobe as the core, acts an important role in the regulation of cognition and behavior, the integration of perception and memory information, and working memory [50]. The MFG and IFG are responsible for executive cognitive function and working memory. The present research found that SCD showed increased DFC variability in left MFG compared to HC while aMCI showed decreased DFC variability in right MFG compared to SCD. This might reveal that the DFC variability decreased as the AD spectrum progresses, representing a gradual decline in information processing ability.

Combined with those findings, we can speculate that SCD and aMCI have common and unique disruption in the triple networks. Actually, the triple networks are involved in a wide range of cognitive tasks through direct or indirect means. Disruption of any network of the triple networks will result in aberrant in goal-related stimuli and internal psychological events [20]. Previous research findings suggested that abnormal organization and function of the triple networks were prominent features of neuropsychiatric diseases. However, the specific changes in static FC within the triple networks of SCD and aMCI were not consistent. For example, some researches claimed that aMCI showed increased static FC in SN while several reported disrupted static FC in SN [21, 23, 38]. One possible reason for the inconsistency of the results may be that the FC pattern was dynamic rather than static during the entire rsfMRI scan, leading to different FC patterns in different scan periods [51]. Therefore, our study confirmed that the DFC of the triple networks were disrupted in SCD and aMCI, suggesting DFC analysis can be used as a complement and verification of static FC analysis.

The present study showed observably negatively associations in SCD and aMCI between the altered DFC variability in the left IFG and cognitive domains, including EM and EF. The results demonstrated that the disruption of DFC significantly related to the declined cognition performance in SCD and aMCI. As EM and EF impaired, the DFC variability of SCD and aMCI in left IFG increased. Moreover, it showed a tread that aMCI exhibited a higher DFC variability while its EM and EF impaired compared to SCD. This might mean that the increased DFC variability of left IFG was to compensate for the impairment of EM and EF

in the progression of preclinical AD spectrum. Furthermore, EF refers to the cognitive process of goal-oriented behavior from goal formulation to successful execution and processing of results [52, 53]. The correlation between the altered DFC variability in the left IFG within ECN and EF confirmed the fact that the ECN is widely used to investigate the mechanism of altered EF in patients [54]. Interestingly, SCD and aMCI showed significantly correlation between the altered DFC variability within ECN and EM. A previous study suggested that the EM deficits in aMCI patients were associated with the right DLPFC functional network [55]. Our results provided a new evidence for the interaction between impaired EF and memory impairment. Taken together, the study suggested that DFC in SCD and aMCI were disrupted, which extended the current understanding of functional network, and showed the importance of evaluating changes in dynamic functional connectivity in preclinical AD spectrum.

The most excellent finding in the current study was that the best-fitting model in diagnosing and characterizing SCD and aMCI was based on the multivariable models. They combined altered DFC variability within triple networks and declined cognitive function. It can be seen that the models had the higher AUC values with high sensitivity and specificity compared to models. Especially, the model was highly specific for aMCI with 98.2% specificity, so the risk of false-positive error is very low, suggesting that the DFC analysis could be a reliable potential biomarker for diagnosing aMCI patients. Specifically speaking, the DFC variability of left putamen played a vital role in the diagnosis of SCD while the DFC variability of right AG played a major role in the diagnosis of aMCI for their higher AUC values. Meanwhile, the DFC variability of right MFG and left IFG acted dominant roles in the differentiation of SCD and aMCI. Those might provide additional information in the research of specific braIn region changes in the SCD and aMCI. Additionally, researches indicated that the classification accuracy of static FC was lower than DFC because time-averaged analysis could not account for microscopic changes of brain states [34, 56, 57]. Studies have shown that DFC contain significantly more behavioral information than static FC [34, 58]. In a word, such reliable methods will have tremendous value for early detection of AD-related pathology.

Limitations

Several limitations of the present study showed be mentioned. Firstly, the patient sample was small, which may have reduced the generalizability of results. In order to avoid this problem, we applied nonparametric permutation test to control the false positive rate. Moreover, our research group are continuously recruiting new volunteers and the NBH-ADsnp database is constantly updated, which means we will further verify our conclusions in near future. Secondly, we collected only 8-min data length on each participant in the current study, resulting in inadequate results. We will take advantage of longer fMRI scan times, like several hours, to improve estimates of DFC variability in the future study. Lastly, the lack of longitudinal researches made it impossible to explore disease transformation in depth. Our research team is following up the recruited volunteers regularly, and we believe that we will further explore the longitudinal changes in DFC in the near future.

Conclusion

The current study revealed common and specific DFC variability abnormalities within the triple networks of SCD and aMCI. Moreover, altered DFC variability of left IFG within ECN was significantly correlated with cognitive decline, including EM and EF. More importantly, the best-fitting models in diagnosing and differentiating SCD and aMCI were multivariable model that combined altered DFC variability (right MTG, left putamen, left insula, and left MFG in distinguishing SCD and HC; right AG, right SFG, and left putamen in distinguishing aMCI and HC; right MFG and left IFG in distinguishing SCD and aMCI) with declined cognitive function. Therefore, our findings suggested that the DFC variability analysis combined the triple-network model can be used as a potential biomarkers of preclinical AD spectrum and may help us to understand abnormal cognitive functions.

Declarations

DATA AVAILABILITY STATEMENT

The datasets analyzed in this manuscript are not publicly available. Requests to access the datasets should be directed to ericcst@aliyun.com.

ETHICS STATEMENT

The studies involving human participants were reviewed and approved by the responsible Human Participants Ethics Committee of the Affiliated Brain Hospital of Nanjing Medical University. The patients/participants provided their written informed consent to participate in this study. Written informed consent was obtained from the individual(s) for the publication of any potentially identifiable images or data included in this article.

AUTHOR CONTRIBUTIONS

CXu, CXi and JC: designed the study. CXu, CXi, JC, QY, GH, HG, and JR: collected the data. CXu: analyzed the data and prepared the manuscript.

FUNDING

This study was supported by the National Natural Science Foundation of China (No. 81701675); the Key Project supported by Medical Science and technology development Foundation, Nanjing Department of Health (No. JQX18005); the Cooperative Research Project of Southeast University-Nanjing Medical University (No. 2018DN0031); the Key Research and Development Plan (Social Development) Project of

Jiangsu Province (No. BE2018608); the Innovation and Entrepreneurship Training Program for College Students in Jiangsu Province (No.201810312061X; 201910312035Z).

COMPETING INTERESTS

The authors declare that they have no competing financial interests.

SUPPLEMENTARY MATERIAL

Please see the supplementary material.

References

1. Jessen F, et al. A conceptual framework for research on subjective cognitive decline in preclinical Alzheimer's disease. Alzheimers Dement. 2014;10(6):844–52.
2. Jessen F, et al. AD dementia risk in late MCI, in early MCI, and in subjective memory impairment. Alzheimers Dement. 2014;10(1):76–83.
3. Xue C, et al., *Distinct Disruptive Patterns of Default Mode Subnetwork Connectivity Across the Spectrum of Preclinical Alzheimer's Disease*. Frontiers in Aging Neuroscience, 2019. 11.
4. Morris JC, Cummings J. Mild cognitive impairment (MCI) represents early-stage Alzheimer's disease. J Alzheimers Dis. 2005;7(3):235–9. discussion 255 – 62.
5. Mitchell AJ, et al. Risk of dementia and mild cognitive impairment in older people with subjective memory complaints: meta-analysis. Acta Psychiatr Scand. 2014;130(6):439–51.
6. Slot RER, et al. Subjective cognitive decline and rates of incident Alzheimer's disease and non-Alzheimer's disease dementia. Alzheimers Dement. 2019;15(3):465–76.
7. Bischkopf J, Busse A, Angermeyer MC. Mild cognitive impairment–a review of prevalence, incidence and outcome according to current approaches. Acta Psychiatr Scand. 2002;106(6):403–14.
8. Chen J, et al. Predicting progression from mild cognitive impairment to Alzheimer's disease on an individual subject basis by applying the CARE index across different independent cohorts. Aging. 2019;11(8):2185–201.
9. Zhang D, Raichle ME. Disease and the brain's dark energy. Nat Rev Neurol. 2010;6(1):15–28.
10. Li SJ, et al. Alzheimer Disease: evaluation of a functional MR imaging index as a marker. Radiology. 2002;225(1):253–9.
11. Menon V. Large-scale brain networks and psychopathology: a unifying triple network model. Trends Cogn Sci. 2011;15(10):483–506.

12. Zhan Y, et al. Longitudinal Study of Impaired Intra- and Inter-Network Brain Connectivity in Subjects at High Risk for Alzheimer's Disease. J Alzheimers Dis. 2016;52(3):913–27.
13. Joo SH, Lim HK, Lee CU. Three Large-Scale Functional Brain Networks from Resting-State Functional MRI in Subjects with Different Levels of Cognitive Impairment. Psychiatry Investigation. 2016;13(1):1–7.
14. Broyd SJ, et al. Default-mode brain dysfunction in mental disorders: A systematic review. Neurosci Biobehav Rev. 2009;33(3):279–96.
15. Raichle ME, et al. A default mode of brain function. Proc Natl Acad Sci U S A. 2001;98(2):676–82.
16. Liang X, et al. Topologically Reorganized Connectivity Architecture of Default-Mode, Executive-Control, and Salience Networks across Working Memory Task Loads. Cereb Cortex. 2016;26(4):1501–11.
17. Sridharan D, Levitin DJ, Menon V. A critical role for the right fronto-insular cortex in switching between central-executive and default-mode networks. Proc Natl Acad Sci U S A. 2008;105(34):12569–74.
18. Uddin LQ. Salience processing and insular cortical function and dysfunction. Nat Rev Neurosci. 2015;16(1):55–61.
19. Menon V, Uddin LQ. Saliency, switching, attention and control: a network model of insula function. Brain Struct Funct. 2010;214(5–6):655–67.
20. Wu X, et al. A Triple Network Connectivity Study of Large-Scale Brain Systems in Cognitively Normal APOE4 Carriers. Front Aging Neurosci. 2016;8:231.
21. He XX, et al. Abnormal salience network in normal aging and in amnestic mild cognitive impairment and Alzheimer's disease. Hum Brain Mapp. 2014;35(7):3446–64.
22. Li CX, et al. Abnormal Brain Network Connectivity in a Triple-Network Model of Alzheimer's Disease. Journal of Alzheimers Disease. 2019;69(1):237–52.
23. Brier MR, et al. Loss of intranetwork and internetwork resting state functional connections with Alzheimer's disease progression. J Neurosci. 2012;32(26):8890–9.
24. Chand GB, et al. Interactions of the Salience Network and Its Subsystems with the Default-Mode and the Central-Executive Networks in Normal Aging and Mild Cognitive Impairment. Brain Connect. 2017;7(7):401–12.
25. Chang C, Glover GH. Time-frequency dynamics of resting-state brain connectivity measured with fMRI. Neuroimage. 2010;50(1):81–98.
26. Preti MG, Bolton TA, Van De Ville D. The dynamic functional connectome: State-of-the-art and perspectives. Neuroimage. 2017;160:41–54.
27. Hutchison RM, et al. Dynamic functional connectivity: promise, issues, and interpretations. Neuroimage. 2013;80:360–78.
28. Finc K, et al. Dynamic reconfiguration of functional brain networks during working memory training. Nat Commun. 2020;11(1):2435.

29. Long Y, et al. Psychological resilience negatively correlates with resting-state brain network flexibility in young healthy adults: a dynamic functional magnetic resonance imaging study. Ann Transl Med. 2019;7(24):809.
30. Lei B, et al., *Diagnosis of early Alzheimer's disease based on dynamic high order networks.* Brain Imaging Behav, 2020.
31. Gu Y, et al. Abnormal dynamic functional connectivity in Alzheimer's disease. CNS Neurosci Ther. 2020;26(9):962–71.
32. Cordova-Palomera A, et al., *Disrupted global metastability and static and dynamic brain connectivity across individuals in the Alzheimer's disease continuum*. Scientific Reports, 2017. 7.
33. Niu H, et al. Abnormal dynamic functional connectivity and brain states in Alzheimer's diseases: functional near-infrared spectroscopy study. Neurophotonics. 2019;6(2):025010.
34. Dong G, et al. Dynamic network connectivity predicts subjective cognitive decline: the Sino-Longitudinal Cognitive impairment and dementia study. Brain Imaging Behav. 2020;14(6):2692–707.
35. Chen J, et al. Differential contributions of subregions of medial temporal lobe to memory system in amnestic mild cognitive impairment: insights from fMRI study. Sci Rep. 2016;6:26148.
36. Chen J, et al. rTMS modulates precuneus-hippocampal subregion circuit in patients with subjective cognitive decline. Aging. 2020;13(1):1314–31.
37. Wotruba D, et al. Aberrant coupling within and across the default mode, task-positive, and salience network in subjects at risk for psychosis. Schizophr Bull. 2014;40(5):1095–104.
38. Chen J, et al. Convergent and divergent intranetwork and internetwork connectivity patterns in patients with remitted late-life depression and amnestic mild cognitive impairment. Cortex. 2016;83:194–211.
39. Lin SJ, et al. Education, and the balance between dynamic and stationary functional connectivity jointly support executive functions in relapsing-remitting multiple sclerosis. Hum Brain Mapp. 2018;39(12):5039–49.
40. Ma WY, et al. Dysfunctional Dynamics of Intra- and Inter-network Connectivity in Dementia With Lewy Bodies. Front Neurol. 2019;10:1265.
41. Xue C, et al. Disrupted Patterns of Rich-Club and Diverse-Club Organizations in Subjective Cognitive Decline and Amnestic Mild Cognitive Impairment. Front Neurosci. 2020;14:575652.
42. Marusak HA, et al. Dynamic functional connectivity of neurocognitive networks in children. Hum Brain Mapp. 2017;38(1):97–108.
43. Rodriguez-Vieitez E, et al. Diverging longitudinal changes in astrocytosis and amyloid PET in autosomal dominant Alzheimer's disease. Brain. 2016;139(Pt 3):922–36.
44. Bellebaum C, et al. Focal basal ganglia lesions are associated with impairments in reward-based reversal learning. Brain. 2008;131(Pt 3):829–41.
45. Looi JC, et al. Differential putaminal morphology in Huntington's disease, frontotemporal dementia and Alzheimer's disease. Aust N Z J Psychiatry. 2012;46(12):1145–58.

46. de Jong LW, et al. Strongly reduced volumes of putamen and thalamus in Alzheimer's disease: an MRI study. Brain. 2008;131(Pt 12):3277–85.
47. Ren P, et al. Longitudinal Alteration of Intrinsic Brain Activity in the Striatum in Mild Cognitive Impairment. J Alzheimers Dis. 2016;54(1):69–78.
48. Lin F, et al. Insula and Inferior Frontal Gyrus' Activities Protect Memory Performance Against Alzheimer's Disease Pathology in Old Age. J Alzheimers Dis. 2017;55(2):669–78.
49. Cohen AD, et al. Basal cerebral metabolism may modulate the cognitive effects of Abeta in mild cognitive impairment: an example of brain reserve. J Neurosci. 2009;29(47):14770–8.
50. Petersen N, et al. Resting-state functional connectivity in women with PMDD. Transl Psychiatry. 2019;9(1):339.
51. Wang J, et al. Abnormal dynamic functional network connectivity in unmedicated bipolar and major depressive disorders based on the triple-network model. Psychol Med. 2020;50(3):465–74.
52. Diamond A. Executive functions. Annu Rev Psychol. 2013;64:135–68.
53. Miller EK, Cohen JD. An integrative theory of prefrontal cortex function. Annu Rev Neurosci. 2001;24:167–202.
54. Brown CA, et al. Distinct patterns of default mode and executive control network circuitry contribute to present and future executive function in older adults. Neuroimage. 2019;195:320–32.
55. Yuan BY, et al. Mediation of episodic memory performance by the executive function network in patients with amnestic mild cognitive impairment: a resting-state functional MRI study. Oncotarget. 2016;7(40):64711–25.
56. Bassett DS, et al. Task-based core-periphery organization of human brain dynamics. PLoS Comput Biol. 2013;9(9):e1003171.
57. Allen EA, et al. Tracking whole-brain connectivity dynamics in the resting state. Cereb Cortex. 2014;24(3):663–76.
58. Liegeois R, et al. Resting brain dynamics at different timescales capture distinct aspects of human behavior. Nat Commun. 2019;10(1):2317.

Tables

Table 1

Demographics and clinical measures of three groups, including SCD, aMCI, and HC

	HC(58)	SCD(44)	aMCI(49)	F values(χ^2)	P values
Age(years)	63.328±6.28	66.000±7.80	63.633±7.58	1.966	0.144
Gender(male/female)	25/33	8/36	13/36	7.865	0.020
Education level(years)	12.40±2.52	12.33±2.59	10.99±2.95*	4.359	0.014[a]
MMSE scores	28.62±1.24	28.34±1.14	27.22±1.86***/**	13.319	<0.001[ab]
MDRS-2	141.57±2.21	139.89±3.61	136.80±5.10***/***	11.808	<0.001[ab]
MoCA	25.11±2.52	24.64±1.95	22.77±2.98***/**	21.740	<0.001[ab]
SCD-Q	3.51±1.52	6.45±0.89***	5.02±1.92***/***	46.568	<0.001[cab]
Composite Z scores of each cognitive domain					
Episodic memory	0.185±0.080	0.330±0.093	-0.519±0.090***/***	25.178	<0.001[ab]
Information processing speed	0.190±0.084	0.042±0.098	-0.264±0.095**	6.339	0.002[a]
Executive function	0.175±0.065	0.147±0.076	-0.330±0.074***/***	15.166	<0.001[ab]
Visuospatial function	0.068±0.098	0.226±0.114	-0.218±0.111*	3.954	0.021[b]

Numbers are given as means ± standard deviation, SD unless stated otherwise. Values for age derived from ANOVA; gender from chi-square test; all clinical measures from ANOVA with age, gender, years of education as covariates. MMSE, Mini-Mental State Examination; MDRS-2, Mattis Dementia Rating Scale-2; MoCA, the Montreal Cognitive Assessment test; SCD-Q, Subjective Cognitive Decline Questionnaire; [a], *post-hoc* analyses showed a significantly group difference between aMCI and HC; [b], *post-hoc* analyses showed a significantly group difference between aMCI and SCD; [c], *post-hoc* analyses showed a significantly group difference between SCD and HC; *, $p < 0.05$; **, $p < 0.01$;***, $p < 0.001$; aMCI, amnestic mild cognitive impairment; SCD, subjective cognitive decline; HC, healthy control.

Table 2

The difference of dynamic functional connectivity variability in default mode network across three groups

Region(aal)	Peak MNI coordinate			F/t	Cluster number
	x	y	z		
:erior default mode network					
OVA					
arahippocampal gyrus	21	-18	-30	6.3284	20
ıferior frontal gyrus	36	24	-24	7.0609	42
nterior cingulum gyrus	-6	39	3	8.9345	22
audate	-9	6	-3	7.232	38
ngular gyrus/superior temporal gyrus	60	-51	21	6.6394	79
uperior frontal gyrus	21	39	27	7.4796	40
ıperior frontal gyrus	-21	33	54	7.2538	21
CI vs HC					
ngular gyrus	42	-51	24	-3.0653	18
uperior frontal gyrus	24	39	33	-3.6477	18
:terior default mode network					
OVA					
ıiddle temporal gyrus	66	-45	-3	6.9386	21
D vs HC					
ıiddle temporal gyrus	-60	-51	-18	-3.942	96
ience network					
OVA					
Hippocampus	39	-27	6	3.8555	20
uperior temporal gyrus	51	-24	6	3.1027	34
ippocampus	-18	-18	-15	6.3901	49
ıferior frontal gyrus	45	39	-6	7.1029	47
ısula/putamen	-45	12	3	11.4039	252
ıperior temporal gyrus	-48	-39	18	6.4033	57
ıferior frontal gyrus	45	15	15	6.6237	28
D vs HC					
utamen	-30	-3	-3	3.6342	15
ısula	-45	12	3	4.1688	53
CI vs HC					
utamen	-27	12	-3	4.0464	11
ecutive control network					
OVA					
ıiddle frontal gyrus	33	54	9	7.1346	38
ıferior frontal gyrus	-39	9	24	6.3027	59
ıiddle frontal gyrus	45	36	21	5.0147	64

iddle frontal gyrus	-42	45	18	7.732	39
ıferior parietal lobule	54	-42	42	8.0083	32
D vs HC					
iddle frontal gyrus	-48	42	21	3.8698	22
CI vs HC					
iddle frontal gyrus	30	57	6	-3.3649	11
ıferior frontal gyrus	-36	15	15	3.7362	14

The x, y, z coordinates is the primary peak locations in the MNI space. Cluster size > 19 voxels in ANOVA analysis, $p < 0.05$; Cluster size > 10 voxels in *post-hoc* test, $p < 0.05$, TFCE-FWE corrected; L, left; R, right; B, bilateral; aMCI, amnestic mild cognitive impairment; SCD, subjective cognitive decline; HC, healthy control.

Figures

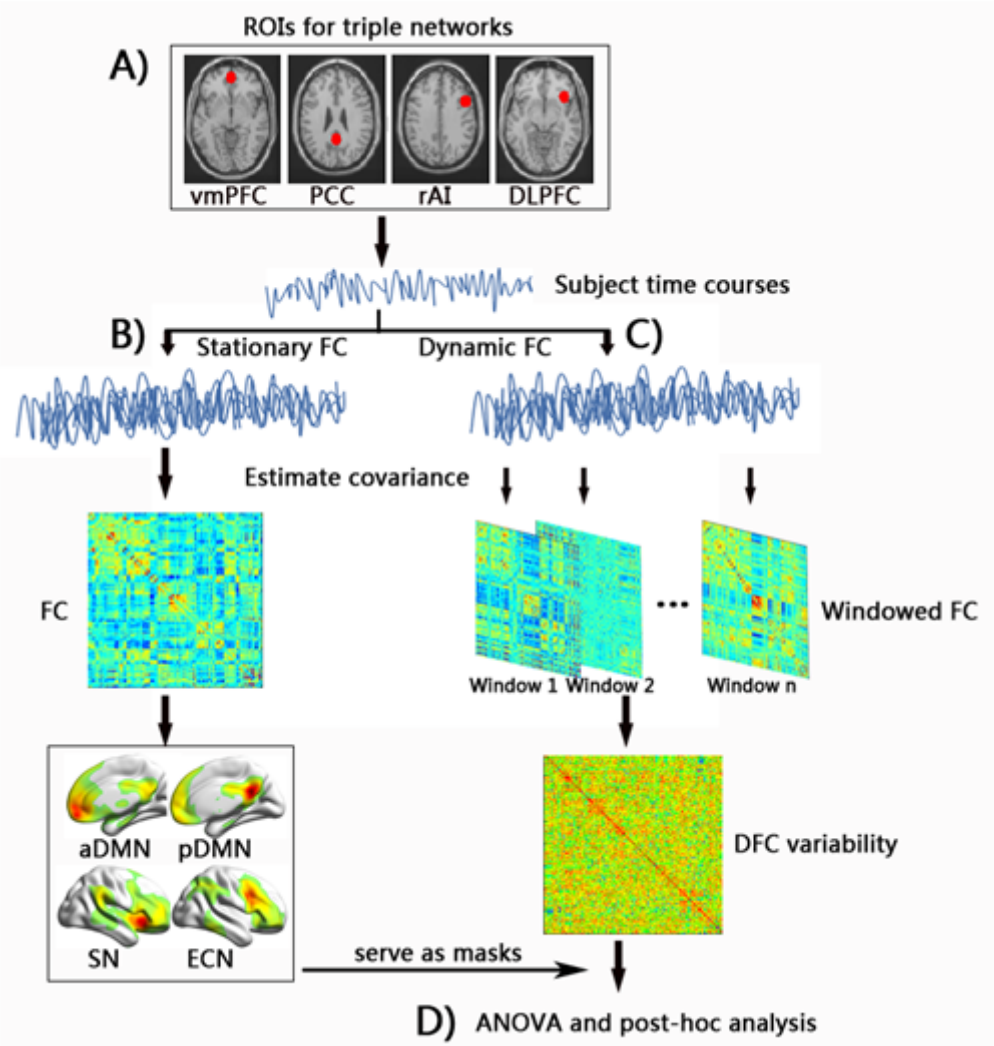

Figure 1

Flowchart for the dynamic functional connectivity analysis in this study. A) For the RS-fMRI data of all subjects, we first used four ROIs to prepare for the next seed-based functional connectivity analysis. B) Then we adopted the stationary functional connectivity analysis and earned the template of the triple networks. C) We applied sliding window approach to analyze the dynamic functional connectivity for the obtained 96 windows. Afterwards, we calculated the dynamic functional connectivity variability across windows. D) At last, we performed statistical analysis. ROI, regions of interests; vmPFC, ventromedial prefrontal cortex; PCC, posterior cingulated cortex; rAI, right anterior insula; DLPFC, dorsolateral prefrontal cortex; FC, functional connectivity; DFC, dynamic functional connectivity; aDMN, anterior default mode network; pDMN, posterior default mode network; SN, salience network; ECN, executive control network. ANOVA, analysis of variance.

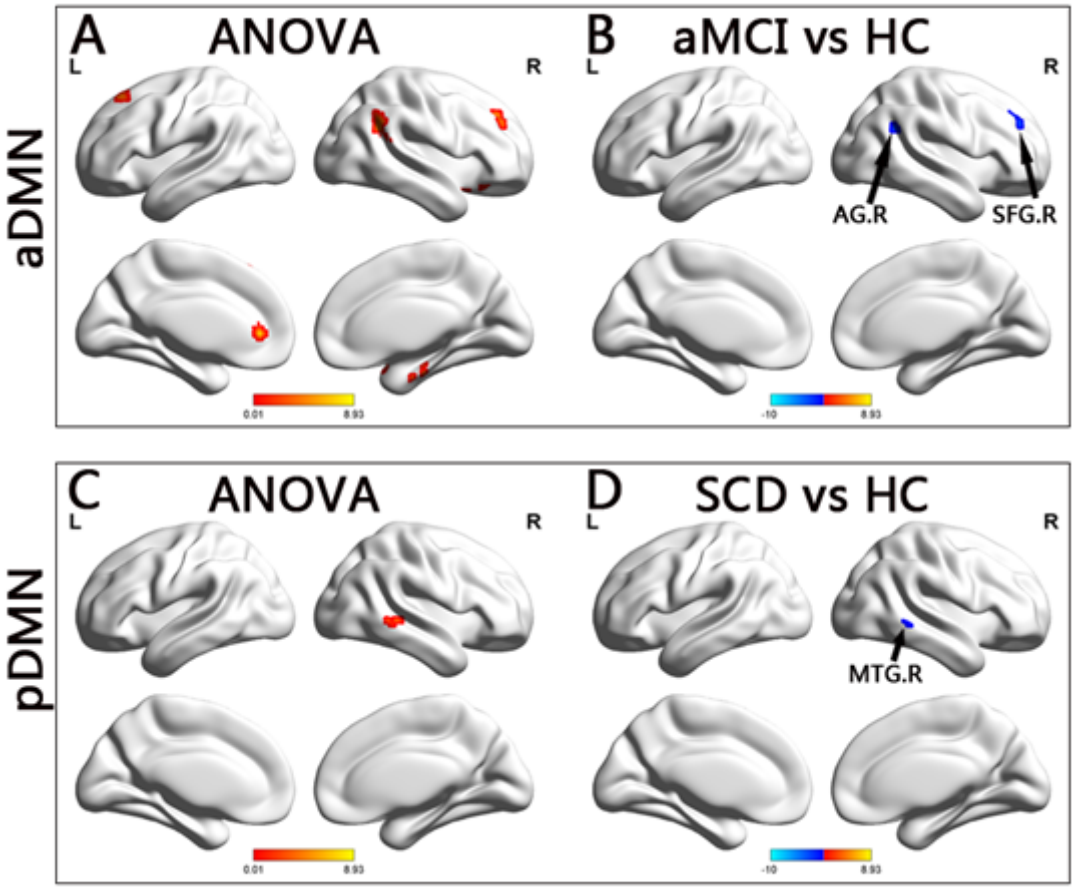

Figure 2

Brain regions exhibiting significant differences in dynamic functional connectivity variability within default mode network. (A, C) Brain regions showing significant differences in dynamic functional connectivity variability within the anterior default mode network and posterior default mode network across three groups, including SCD, aMCI, and HC ($p < 0.05$, the cluster size > 19 voxels). (B, D) Results of post-hoc analysis in voxel-wise analysis (TFCE-FWE corrected, cluster size > 9, $p < 0.05$). aDMN, anterior default mode network; pDMN, posterior default mode network; aMCI, amnestic mild cognitive impairment;

SCD, subjective cognitive decline; HC, healthy controls; AG, angular gyrus; SFG, superior frontal gyrus; MTG, middle temporal gyrus; R, right.

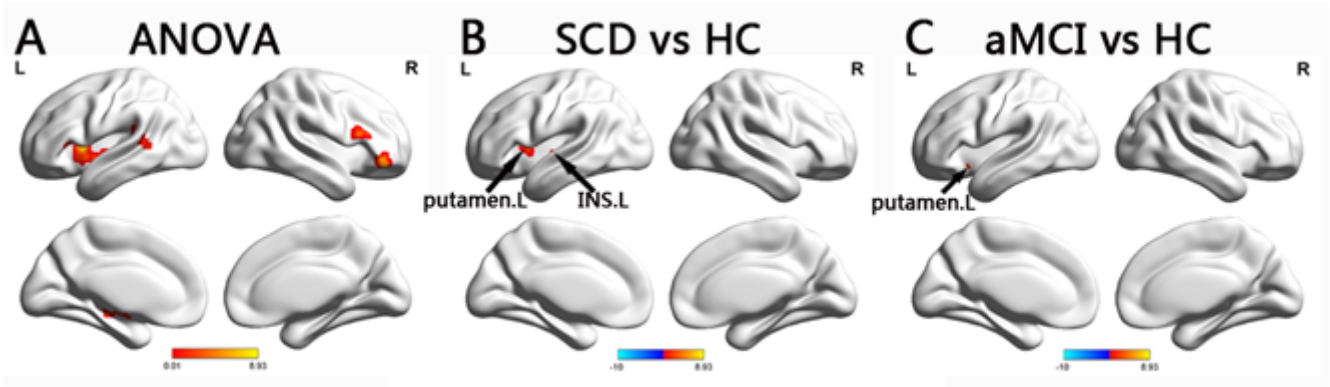

Figure 3

Brain regions exhibiting significant differences in dynamic functional connectivity variability within salience network. (A) Brain regions showing significant differences in dynamic functional connectivity variability within the salience network across three groups, including SCD, aMCI, and HC ($p < 0.05$, the cluster size > 19 voxels). (B-C) Results of post-hoc analysis in voxel-wise analysis (TFCE-FWE corrected, cluster size > 9, $p < 0.05$). aDMN, anterior default mode network; pDMN, posterior default mode network; aMCI, amnestic mild cognitive impairment; SCD, subjective cognitive decline; HC, healthy controls; INS, insula; L, left.

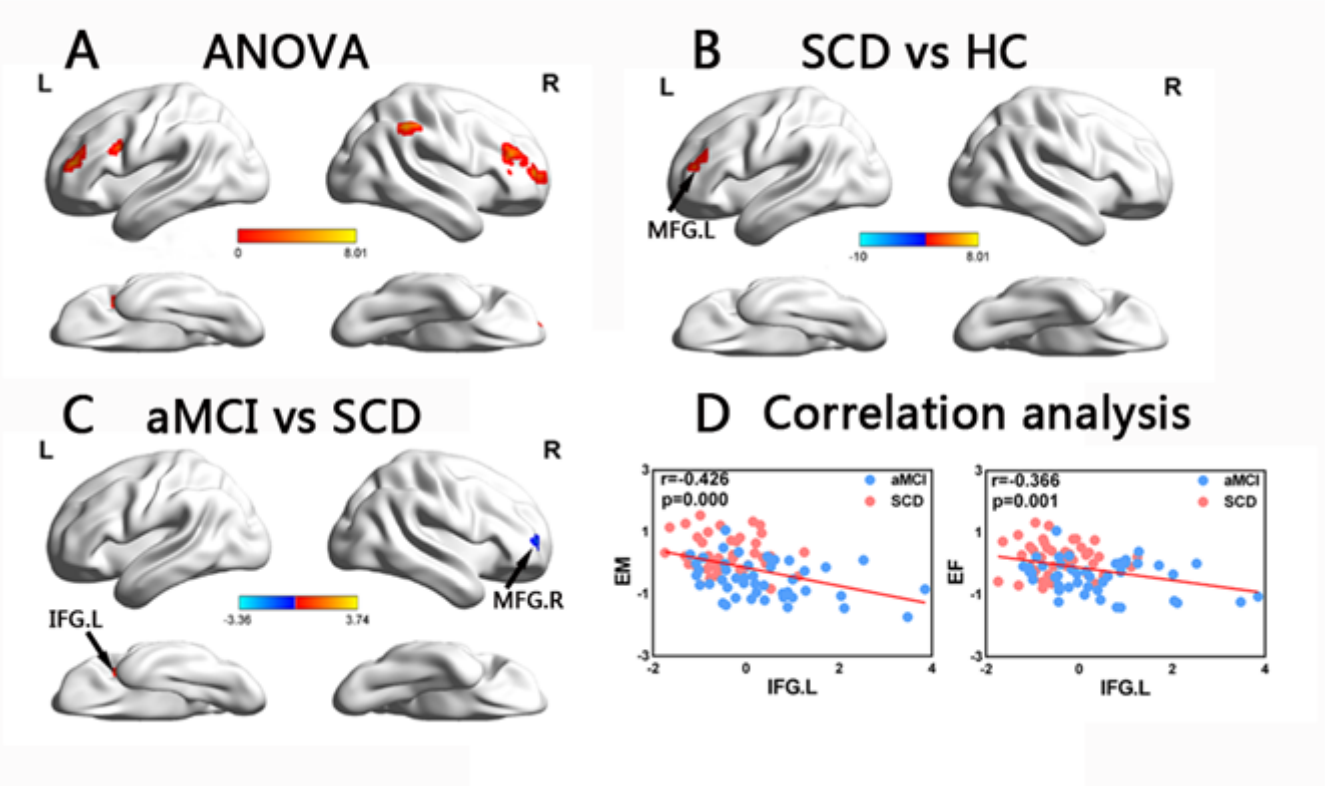

Figure 4

Brain regions exhibiting significant differences in dynamic functional connectivity variability within executive control network and the correlation with cognitive function. (A) Brain regions showing significant differences in dynamic functional connectivity variability within the executive control network across three groups, including SCD, aMCI, and HC ($p < 0.05$, the cluster size > 19 voxels). (B-C) Results of post-hoc analysis in voxel-wise analysis (TFCE-FWE corrected, cluster size > 9, $p < 0.05$). (D) Results of associations between altered dynamic functional connectivity variability and cognitive function. Age, gender, and years of education were used as covariates of results (Bonferroni corrected, $p < 0.05$). aDMN, anterior default mode network; pDMN, posterior default mode network; aMCI, amnestic mild cognitive impairment; SCD, subjective cognitive decline; HC, healthy controls; MFG, middle frontal gyrus; IFG, inferior frontal gyrus; EM, episodic memory; EF, executive function; R, right; L, left.

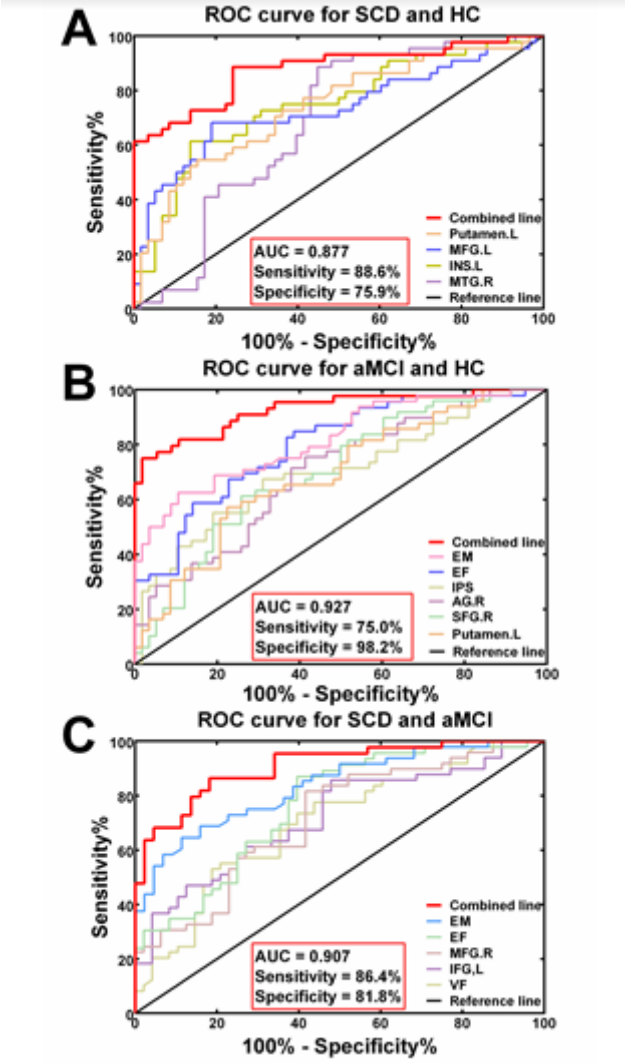

Figure 5

Diagnosis and differentiation of SCD and aMCI based on ROC analysis. (A) ROC curve showing the classification of SCD and HC; (B) ROC curve showing the classification of aMCI and HC; (C) ROC curve showing the classification of aMCI and SCD.

Supplementary Files

This is a list of supplementary files associated with this preprint. Click to download.

- SupportingInformation.doc